Electromechanical Energy Conversion Systems (EECS)
Niroo Research Institute (NRI)
Vol. 4, No. 1, Spring 2025, pp. 48- 52
DOI: 10.30503/EECS.2025.494806.1069
Original Article

A Configuration of Wound Mover Linear Resolver for Compensating Edge Effect

Fateme Zare[1*], Farid Tootoonchian[2]

Abstract

Resolvers are essential position sensors used for determining rotational and linear motion. However, in linear resolvers, longitudinal and lateral end effects reduce positioning accuracy, posing a significant challenge. To mitigate these effects, implementing compensation methods is crucial. One effective approach involves using a tubular structure instead of a flat structure. The tubular design eliminates the lateral end effect, also known as the edge effect, leading to improved accuracy and performance. This paper proposes a tubular structure for a wound mover resolver to address these challenges. The proposed design minimizes the impact of end effects and enhances sensor precision. To validate its performance, finite element simulations and experimental tests were conducted. The results confirm the effectiveness of the tubular resolver design, demonstrating improved accuracy and reduced positioning errors compared to conventional flat structures. These findings highlight the advantages of the tubular structure, making it a promising solution for high-accuracy resolver applications.

Keywords: Wound mover resolver, linear resolver, tubular resolver, lateral end effect, edge effect

Received Date: 2024-12-19; Revised Date: 2025-02-09; Accepted Date:2025-04-28

1. INTRODUCTION

Position sensors play a critical role in modern control systems. Among these, resolvers have emerged as one of the most prominent and widely studied position sensors in recent years. While resolvers have a higher initial cost compared to their primary competitor, encoders, they offer excellent performance in industrial environments, demonstrating strong resistance to noise and temperature variations [1]. As a result, they are extensively used across various industries.

Resolvers are typically categorized into two main types based on their rotor structure: wound rotor and variable reluctance. In wound rotor resolvers, both the stator and rotor contain windings, with excitation and signal windings placed accordingly. In contrast, variable reluctance resolvers lack rotor windings, and changes in reluctance arise due to the rotor's shape. These changes in reluctance occur as a result of variations in either the air gap length or the cross-sectional area, based on the principles of magnetic reluctance [2].

Based on the type of motion, resolvers are classified into two main categories: rotary and linear resolvers, which are used to determine position in rotational and linear movements, respectively. The design challenges of a linear resolver with a wound mover were presented in [3], where the structure was flat with a short moving part. Analytical modeling, structural optimization, and performance evaluation under various mechanical error conditions were discussed in [4]–[6].

Subsequently, variable reluctance linear resolvers were introduced. In [8], a variable reluctance linear resolver with a varying cross-sectional area was proposed, and its performance was analyzed using finite element simulations. In [9], the performance of this resolver was examined using the winding function method, which requires significantly less computation time than finite element simulations. This method was further utilized to propose a solution for compensating end effects. In [10], a flat variable reluctance linear resolver with a varying air-gap length was introduced, and its performance was evaluated through finite element simulations. Later, studies in [11]–[13] explored the modeling of flat variable reluctance linear resolvers with air-gap variations using the winding function or equivalent magnetic circuit methods.

As with other linear machines, the end effect in all these linear resolvers contributes to increased errors and reduced accuracy. This end effect in flat linear machines includes both longitudinal and transverse components, caused by asymmetry in the equivalent magnetic circuit.

In this paper, a tubular structure for a linear resolver with a wound mover is proposed. This design eliminates the transverse end effect, significantly enhancing positioning accuracy. Simulation results confirm the effectiveness of

[1] Department of *Electrical and Computer Engineering, Isfahan University of Technology, Isfahan, Iran*
[2] *Department of Electrical Engineering, Iran University of Science and Technology, Tehran, Iran*
**Corresponding author, Email: fzare@iut.ac.ir*

the proposed resolver, and experimental results further validate its improved performance.

2. Tubular Wound Mover Resolver

In tubular linear machines, both the stator and the moving part feature cylindrical structures. Depending on the machine's design, either coils or magnets are mounted on these components. The structure of the tubular resolver, which consists of an outer long stator and an inner wound moving part, is illustrated in Fig. 1.

As shown in Fig. 1(a), the stator of this resolver is a hollow cylinder with horizontal slots on its inner surface. The sin and cos signal coils are arranged in the form of horizontal discs within these slots. The moving part, depicted in Fig. 1(b), is short, cylindrical, and positioned inside the stator. Its outer surface contains disc-shaped slots for housing the excitation coils.

In the proposed resolver, each section of the stator includes 6 slots, which are aligned with 8 slots on the moving part. In the long stator configuration, the 6-slot pattern can be repeated multiple times, allowing the stator length to exceed that of the moving part. Conversely, in a long moving part configuration, the stator length remains limited to 6 slots, while the 8-slot pattern on the moving part is repeated.

It is also worth noting that the tubular resolver can be designed with either an external stator or an internal stator.

Fig. 2(a) illustrates the stator winding configuration. As shown, the *cos* coils are placed in all the slots, but with varying numbers of turns. The *sin* signal coils, on the other hand, have an equal number of turns, with their winding direction being positive in the second and third slots and negative in the fifth and sixth slots.

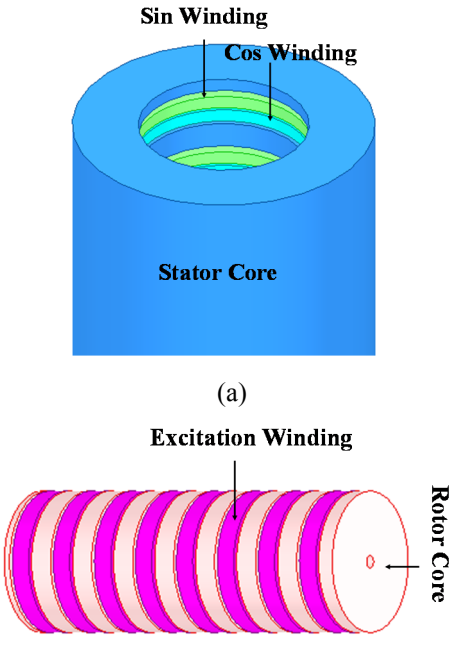

Fig. 1: Linear Tubular Resolver a) Long stator b) Short movable part

Fig. 2(b) depicts the excitation winding configuration. In this figure, the excitation winding is designed as a tooth-wound coil with a variable number of turns. In this resolver, the stator core and the moving part are made of ferromagnetic sheet material. Table 1 shows the dimensions of the designed resolver.

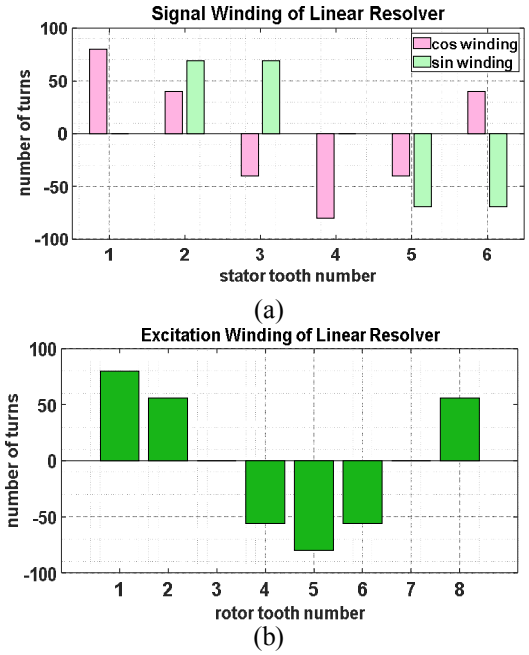

Fig. 2: Winding of Linear Tubular Resolver a) Stator b) Movable part

Table 1: Physical dimension of proposed resolver

Stator length	30 mm
Stator Outer/ Inner Diameter	23 / 13 mm
Stator Outer/ inner Diameter	11 / 5 mm
Stator / Mover teeth	6 / 8
Mover slot height	2 mm
Mover slot width	1.3 mm
Stator slot height	3 mm
Stator slot width	1.5 mm

In the design of a resolver as a position sensor, the primary goal is to minimize its dimensions as much as possible. However, manufacturing constraints must also be carefully considered. It is important to note that, unlike electrical machines, the minimum physical dimensions of resolvers are generally not dictated by magnetic saturation, as saturation in resolvers is quite rare. Instead, the minimum dimensions are typically determined by mechanical strength requirements and the practical considerations for sensor assembly and winding.

The simulation results of the designed resolver will be analyzed further using the finite element method.

3. Finite element analysis

For the finite element simulation, the commercial software Ansys Electronics Desktop Maxwell Design is used. It is

important to note that the guidelines for the finite element simulation of resolvers, as described in [14], are followed.

A sinusoidal supply voltage with a frequency of 4 kHz is applied to the excitation winding. The induced voltages in the sin and cos signal windings, which exhibit amplitude modulation, are then calculated. By extracting the peak values of these signals and applying the arctangent function to the ratio of the voltages, the position is determined. The calculated position is subsequently compared with the reference position, which is derived based on the set speed, to compute the position error.

The finite element simulation of the resolver under study is conducted in three different scenarios. In the first case, both the stationary and moving parts are assumed to have infinite lengths, and the finite element simulation is performed using Master/Slave boundary conditions. The output signals of the resolver in this scenario are shown in Fig. 3(a). In the second case, the stator is modeled as having a long length, while the mover is short. The corresponding output signals are displayed in Fig. 3(b). In the third case, the stator is short, and the mover is long, with the resulting output voltages shown in Fig. 3(c).

As illustrated in Fig. 3, the peak values of the induced voltage signals in the stator signal windings are proportional to the sine and cosine of the position of the moving part. Fig. 4 shows the peak of the voltage signals from Fig. 3(b), calculated using the Hilbert transform and processed with MATLAB software.

To further assess the performance of the designed resolver, the position detection error is calculated, as shown in Fig. 5. For this evaluation, the position is determined by using the envelope of the calculated signals from Fig. 4. It is worth mentioning that the operation principle of the studied resolver is based on the excitation current applied to the excitation winding:

$$I_e = I_m \cos(\omega t) \tag{1}$$

The voltage equations for the stator windings consider the winding resistance, currents, and flux linkages. Due to the high input impedance of the RDC, the stator currents are negligible.

$$v_{sin} = \frac{d}{dt}(L_{s,e} I_m \cos(\omega t)) \tag{2}$$

$$v_{cos} = \frac{d}{dt}(L_{c,e} I_m \cos(\omega t)) \tag{3}$$

where $L_{s,e}$ and $L_{c,e}$ are mutual inductance between excitation winding and the stator's sine and cosine windings and can be defined as:

$$L_{s,e} = L\sin(\frac{x}{\tau_p} \times \pi) \tag{4}$$

$$L_{c,e} = L\cos(\frac{x}{\tau_p} \times \pi) \tag{5}$$

where τ_p is the pole pitch, L is the maximum value of mutual inductance, and x is the displacement between the stator and mover. Substituting (4)-(5) into (2)-(3) the induced voltages can be obtained as:

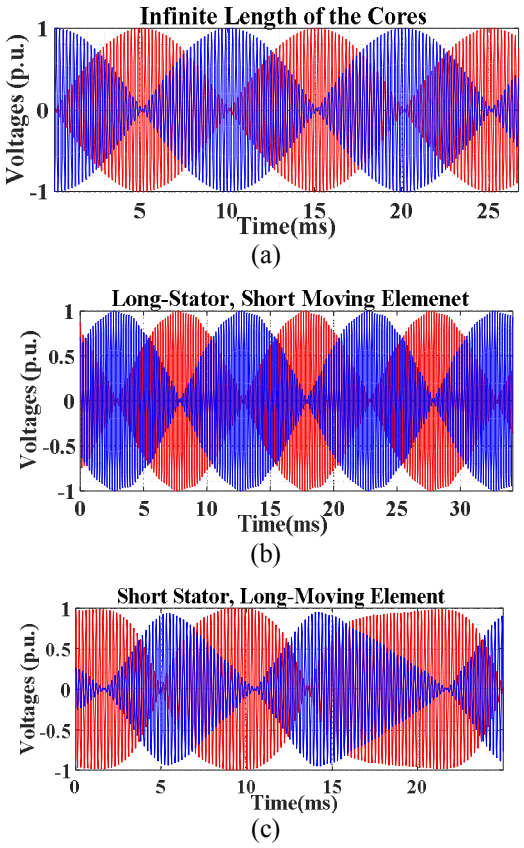

Fig. 3: Induced voltages in the signal windings of the linear tubular resolver: (a) stator and moving part with infinite length, (b) long stator and short moving part, and (c) short stator and long moving part.

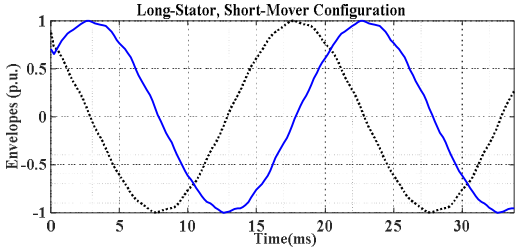

Fig. 4: Envelope of the induced voltage signals in the sine and cosine windings in the case of a long stator and short moving part.

$$v_{sin} = -(LI_m\omega)\sin\left(\frac{\pi}{\tau_p} \times x\right)\sin(\omega t) + (\frac{LI_m\pi}{\tau_p}V_x)\cos(\frac{\pi}{\tau_p}x)\cos(\omega t) \tag{6}$$

$$v_{cos} = -(LI_m\omega)\cos\left(\frac{\pi}{\tau_p} \times x\right)\sin(\omega t) - (\frac{LI_m\pi}{\tau_p}V_x)\sin(\frac{\pi}{\tau_p}x)\cos(\omega t) \tag{7}$$

Because the frequency of the excitation voltage is much higher than the mover speed (V_x), the moving voltage is negligible. So, the induced voltages can be reduced to:

$$v_{sin} = -(LI_m\omega)\sin\left(\frac{\pi}{\tau_p}\times x\right)\sin(\omega t) \quad (8)$$

$$v_{cos} = -(LI_m\omega)\cos\left(\frac{\pi}{\tau_p}\times x\right)\sin(\omega t) \quad (9)$$

Therefore, x can be calculated from the arctangent of the ratio of two-phase voltages:

$$x = \frac{\tau_p}{\pi}\times tan^{-1}\left(\frac{v_{sin}}{v_{cos}}\right) \quad (3)$$

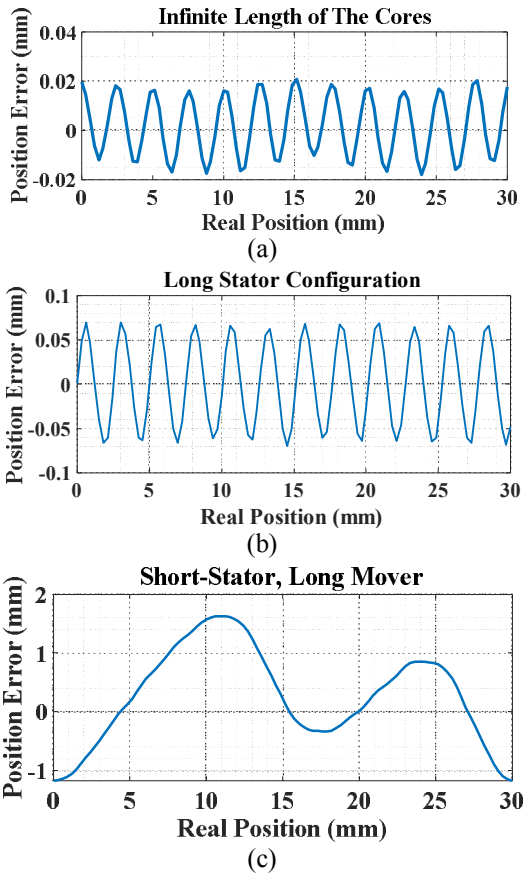

Fig. 5: Positioning error in the linear tubular resolver: a) stator and moving part with infinite length, b) long stator and short moving part, and c) short stator and long moving part.

The position detection error is determined by the difference between the actual position of the resolver, calculated based on time and speed, and the value obtained from Equation (3) as below:

$$error_x = V_x \times t - x \quad (4)$$

where $error_x$ is given the position error and V_x is the linear velocity.

As shown in Fig. (5), the highest accuracy is achieved by the resolver with infinite length stator and mover, which, however, is not practically feasible. When considering actual lengths for the stationary and moving cores, position error increases due to the introduction of longitudinal end effects. If the moving section, which carries the excitation winding, is extended, the flux linkage between parts that are misaligned with the signal winding increases, resulting in a larger position detection error. This is in contrast to the case where the stator is long, and the excitation-carrying moving section is short.

The maximum position error (MPE) and the average of absolute position error (AAPE) for the ideal resolver are 0.02 mm and 0.01 mm, respectively. For the resolver with a long stator and short moving section, the MPE is 0.07 mm, and the AAPE is 0.04 mm. In the case of the resolver with a short stator and a long moving section, the MPE is 1.63 mm, and the AAPE is 0.72 mm. Based on these results, the configuration with a long stator and short moving section is selected for the practical prototype construction.

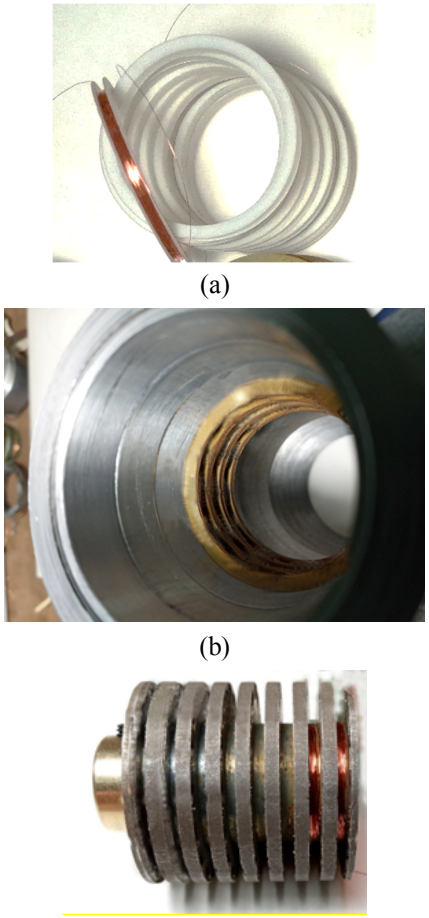

Fig. 6: Prototype resolver: (a) the PVC holder of the stator coils, (b) the assembled stator, and (c) the mover

4. Practical Prototype Construction

To further evaluate the performance of the designed resolver, the construction process has been completed, and experimental results have been assessed. Fig. 6(a) shows the PVC spools used for winding the stator. The ferrite sheets forming the stator core are assembled with these PVC spools to create the stator core. Fig. 6(b) illustrates the assembled stator placed inside the aluminum housing. Fig. 6(c) shows the core of the moving section, along with the excitation windings. To evaluate the performance of the

fabricated prototype, a testing system has been designed and constructed, as shown in Fig. 7. This system includes a function generator that provides the necessary voltage for the excitation winding at a frequency of 4 kHz. A DC motor, along with a mechanism to convert rotational motion to linear motion, is used to generate linear movement. A linear encoder is employed to determine the reference position, while a digital oscilloscope stores the output voltages. The measured output voltages are presented in Fig. 8. Position error calculations using the experimental signals show that the sensor's accuracy is within 10% of the error predicted by the finite element method.

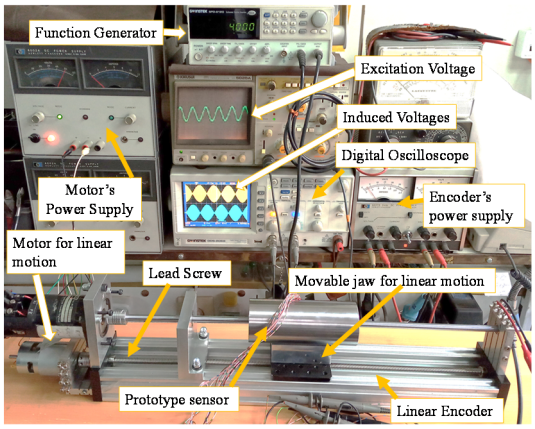

Fig. 7: Test setup for tubular linear resolver

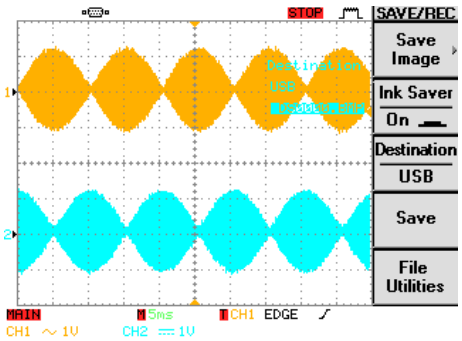

Fig. 8: Induced voltages in sin and cos signal winding

5. Conclusion

Linear resolvers are crucial position sensors used to determine position in linear motion. The limited magnetic circuit, in terms of length and width, results in longitudinal and transverse end effects (edge effects) in linear resolvers. The use of a tubular structure, due to its symmetrical design, eliminates the transverse end effect. This paper proposes a wound tubular resolver and examines the effects of the stator/core and mover/core lengths, comparing them to the case where both stationary and moving parts have infinite lengths. Based on the superior accuracy of the structure with a long stator and short moving part, this configuration was selected for experimental testing. A practical prototype of the sensor, along with the required testing system, was built. A comparison of the experimental results with those obtained from transient finite element simulations confirmed the accuracy of the design and simulation process.

References

[1] X. Ge, Z. Q. Zhu, R. Ren, J. T. Chen "A Novel variable reluctance resolver for HEV/EV applications", *IEEE Trans. Ind. Appl*., Vol. 52, no. 4, pp. 2872 -2880, July-Aug. 2016

[2] M. KhajueeZadeh, F. Zare and Z. Nasiri-Gheidari, "Reliability Analysis of Two Resolver Configurations Under Faulty Conditions in 2DOF System," in *IEEE Transactions on Instrumentation and Measurement*, doi: 10.1109/TIM.2022.3229711.

[3] Z. Nasiri-Gheidari, "Design, Analysis, and Prototyping of a New Wound-Rotor Axial Flux Brushless Resolver", IEEE Transaction on Energy Conversion, vol. 32, no. 1, pp. 276 - 283, 2017

[4] A. Paymozd, H. Saneie, A. Daniar, and Z. Nasiri-Gheidari, "Accurate and Fast Subdomain Model for Electromagnetic Design Purpose of Wound-Field Linear Resolver," in *IEEE Transactions on Instrumentation and Measurement*, vol. 70, pp. 1-8, 2021, Art no. 9003408, doi: 10.1109/TIM.2021.3080400.

[5] A. Paymozd, H. Saneie, Z. Nasiri-Gheidari and F. Tootoonchian, "Subdomain Model for Predicting the Performance of Linear Resolver Considering End Effect and Slotting Effect," in *IEEE Sensors Journal*, vol. 20, no. 24, pp. 14747-14755, 15 Dec.15, 2020, doi: 10.1109/JSEN.2020.3010785.

[6] A. Daniar, Z. Nasiri-Gheidari and F. Tootoonchian, "Position error calculation of linear resolver under mechanical fault conditions," in *iET Science Measurement*, vol. 11, no. 7, pp. 948-954, 2017, doi.org/10.1049/iet-smt.2017.0063

[7] A. Keyvannia and Z. Nasiri-Gheidari, "A Comprehensive Winding Method for Linear Variable-Reluctance Resolvers to Compensate for the End Effects," in *IEEE Transactions on Industrial Electronics*, 2022, doi: 10.1109/TIE.2022.3210572.

[8] M. Bahari and Z. Nasiri-Gheidari, "Longitudinal End Effect in a Variable Area Linear Resolver and its Compensating Methods," *Electrical Engineering (ICEE), Iranian Conference on*, 2018, pp. 1316-1321, doi: 10.1109/ICEE.2018.8472431.

[9] M. Bahari, R. Alipour-Sarabi, Z. Nasiri-Gheidari and F. Tootoonchian, "Proposal of Winding Function Model for Geometrical Optimization of Linear Sinusoidal Area Resolvers," in *IEEE Sensors Journal*, vol. 19, no. 14, pp. 5506-5513, 15 July 15, 2019, doi: 10.1109/JSEN.2019.2908926.

[10] A. Daniar and Z. Nasiri-Gheidari, "The influence of different configurations on position error of linear variable reluctance resolvers," *2017 Iranian Conference on Electrical Engineering (ICEE)*, 2017, pp. 955-960, doi: 10.1109/IranianCEE.2017.7985177.

[11] A. Ramezannezhad, P. Naderi and L. Vandevelde, "A Novel Method for Accuracy Improvement of Variable Reluctance Linear Resolvers," in *IEEE Sensors Journal*, vol. 22, no. 19, pp. 18409-18417, 1 Oct.1, 2022, doi: 10.1109/JSEN.2022.3199807.

[12] P. Naderi, A. Ramezannezhad and L. Vandevelde, "A Novel Linear Resolver Proposal and Its Performance Analysis Under Healthy and Asymmetry Air-Gap Fault," in *IEEE Transactions on Instrumentation and Measurement*, vol. 71, pp. 1-9, 2022, Art no. 9504109, doi: 10.1109/TIM.2022.3155747.

[13] A. Daniar, Z. Nasiri-Gheidari, and F. Tootoonchian, "Performance Analysis of Linear Variable Reluctance Resolvers Based on an Improved Winding Function Approach," in IEEE Transactions on Energy Conversion, vol. 33, no. 3, pp. 1422-1430, Sept. 2018, doi: 10.1109/TEC.2018.2813335.

[14] H. Saneie, R. Alipour-Sarabi, Z. Nasiri-Gheidari, and F. Tootoonchian, "Challenges of Finite Element Analysis of Resolvers", IEEE Trans. On Energy Conversion, vol. 34, no. 2, pp. 973-983, 2018